



Article

A Deep-Learning-Based Method for Extracting an Arbitrary Number of Individual Power Lines from UAV-Mounted Laser Scanning Point Clouds

Sha Zhu ¹, Qiang Li ², Jianwei Zhao ¹, Chunguang Zhang ¹, Guang Zhao ¹, Lu Li ¹, Zhenghua Chen ^{3,*} and Yiping Chen ⁴

¹ State Grid Siji Location Based Service Co., Ltd., Beijing 102200, China; zhaojianwei@sgitg.sgcc.com.cn (J.Z.); zhangchunguang@sgitg.sgcc.com.cn (C.Z.); zhaoguang@sgitg.sgcc.com.cn (G.Z.)

² State Grid Information & Telecommunication Group Co., Ltd., Beijing 102200, China; liqiang@sgitg.sgcc.com.cn

³ Fujian Provincial Key Laboratory of Network Computing and Intelligent Information Processing, Fuzhou University, Fuzhou 350116, China

⁴ School of Geospatial Engineering and Science, Sun Yat-sen University, Zhuhai 519082, China; chenyp79@mail.sysu.edu.cn

* Correspondence: 221027023@fzu.edu.cn

Abstract: In recent years, laser scanners integrated with Unmanned Aerial Vehicles (UAVs) have exhibited great potential in conducting power line inspections in harsh environments. The point clouds collected for power line inspections have numerous advantages over remote image data. However, point cloud-based individual power line extraction, which is a crucial technology required for power line inspections, still poses several challenges such as massive 3D points, imbalanced category points, etc. Moreover, in various power line scenarios, previous studies often require manual setup and careful adjustment of different thresholds to separate different power lines, which is inefficient for practical applications. To handle these challenges, in this paper, we propose a multi-branch network to automatically extract an arbitrary number of individual power lines from point clouds collected by UAV-based laser scanners. Specifically, to handle the massive 3D point clouds in complex outdoor scenarios, we propose to leverage deep neural network for efficient and rapid feature extraction in large-scale point clouds. To mitigate imbalanced data quantities across different categories, we propose to design a weighted cross-entropy loss function to measure the varying importance of each category. To achieve the effective extraction of an arbitrary number of power lines, we propose leveraging a loss function to learn the discriminative features that can differentiate the points belonging to different power lines. Once the discriminative features are learned, the Mean Shift method can distinguish the individual power lines by clustering without supervision. The evaluations are executed on two datasets, which are acquired at different locations with UAV-mounted laser scanners. The proposed method has been thoroughly tested and evaluated, and the results and discussions confirm its outstanding ability to extract an arbitrary number of individual power lines in point clouds.

Keywords: point cloud; UAV-mounted laser scanning system; individual power line extraction; arbitrary number of power lines



Citation: Zhu, S.; Li, Q.; Zhao, J.; Zhang, C.; Zhao, G.; Li, L.; Chen, Z.; Chen, Y. A Deep-Learning-Based Method for Extracting an Arbitrary Number of Individual Power Lines from UAV-Mounted Laser Scanning Point Clouds. *Remote Sens.* **2024**, *16*, 393. <https://doi.org/10.3390/rs16020393>

Academic Editors: Abdul Awal Md Nurunnabi, Meida Chen, Yan Xia and Felicia Norma Rebecca Teferle

Received: 10 November 2023

Revised: 10 December 2023

Accepted: 14 December 2023

Published: 19 January 2024



Copyright: © 2024 by the authors. Licensee MDPI, Basel, Switzerland. This article is an open access article distributed under the terms and conditions of the Creative Commons Attribution (CC BY) license (<https://creativecommons.org/licenses/by/4.0/>).

1. Introduction

At present, conventional methods of power line inspection, such as manual inspection [1] and manned helicopter inspection [2], frequently necessitate the physical presence of personnel at the site for early fault detection and maintenance. However, numerous transmission lines are situated in challenging environments, including hot deserts, mountainous terrains, dense forests, and water bodies, presenting significant obstacles for routine

power line inspections. Moreover, transmission towers in mountainous areas often reach tens to hundreds of meters in height, making it challenging for ground personnel to obtain a clear view of the power lines. Consequently, tower climbing and line inspection for defect detection become imperative, involving the handling of live wires, posing considerable risks and hindering the prompt identification of power line issues. Additionally, these conventional inspection methods are highly susceptible to the influence of terrain and weather conditions. The outcomes of inspections heavily depend on the experience of personnel, resulting in a time-consuming and labor-intensive process [3,4].

In recent years, with the development of sensor technology, remote sensing data has been widely used in power line inspection due to its convenience, safety, and efficiency in data acquisition [5–8]. According to the data acquisition manner, remote sensing data can be classified into the following two categories: image-based data and 3D point-cloud-based data. Image-based data mainly includes Synthetic Aperture Radar (SAR) images and aerial photographs. Point-cloud-based data mainly includes Airborne Laser Scanning (ALS) point cloud data and Mobile Laser Scanning (MLS) point cloud data. Due to the easier accessibility of images, many studies focus on exploiting remote sensing images to accomplish power line inspection [9–11]. Although these studies have shown promising performance in certain scenarios, the performance of these image-based methods is susceptible to issues such as occlusion and lighting variation.

A UAV integrated with laser scanners, as a low-cost type of ALS system, offers a cost-effective solution for rapidly capturing three-dimensional spatial information as point clouds in large-scale scenes [12]. Particularly in remote mountainous areas where it is difficult for personnel to directly access, the UAV-mounted laser scanning systems have exhibited significant potential for practical application. Moreover, compared to optical imaging systems, laser scanning systems have exhibited many advantages, such as precise spatial information collection, real geometry information acquisition, independence from lighting conditions, etc. [13]. Therefore, this paper mainly focuses on utilizing the UAV-mounted laser scanning systems for power line inspection.

Despite of the advantages brought by UAV-mounted laser scanning systems [14], the automated individual extraction of power lines from point clouds for routine power line inspection still poses many challenges. Specifically, on one hand, the differences exist in the spatial distances between different power lines in various scenarios and the number of power lines are inconsistent in different scenarios. Moreover, the power lines in the collected point clouds may become discontinuous or interrupted due to occlusion. Therefore, the robustness and generalization of traditional methods, i.e., clustering-based algorithms [15] or RANSAC model fitting-based algorithms [16], to extract individual power lines in point clouds are heavily influenced when they are applied in different scenarios. This is because they often heavily rely on manual setup and the careful adjustment of different thresholds to separate different power lines. However, the manually set thresholds are challenging to adapt to and extract an uncertain number of power lines in various situations, such as discontinuous power lines and different spatial distances between different power lines. On the one hand, there are massive 3D points in the point clouds collected by UAV-mounted laser scanning systems. A significant category imbalance problem exists in the collected point cloud scenes. Specifically, the number of 3D points for power lines and power towers in the scenes is much smaller than that of other categories. This can lead to the declined performance of the extraction model, where the minority categories, i.e., power towers and power lines, are misclassified as other majority categories.

In order to benefit the routine power line inspection, this paper mainly focuses on proposing a deep-learning-based method to achieve the automated extraction of individual power lines and power towers in point clouds collected by UAV-based laser scanners. Specifically, to handle the massive 3D point clouds in complex outdoor scenarios, we propose to leverage the RandLA-Net [17] as the backbone network for efficient and rapid feature extraction in large-scale point clouds. To mitigate imbalanced data quantities across different categories, we propose to design a weighted cross-entropy loss function to

measure the varying importance of each category. To effectively learn the discriminative features to differentiate the points belonging to different power lines, we propose to design a discriminative loss function to align the point features generated by the neural network. Therefore, we summarize the main contributions of our paper as follows:

1. We propose an end-to-end and multi-branch network named EM-Net to automatically and efficiently extract individual power lines and power towers in point clouds collected by UAV-based laser scanners.
2. In order to effectively extract an arbitrary number of individual power lines, we design a discriminative loss function into the EM-Net to automatically learn about discriminative features for differentiating the points belonging to different power lines. The learned discriminative features can easily be used in traditional unsupervised clustering algorithms to extract an arbitrary number of individual power lines.
3. To assess the accuracy and robustness of our proposed EM-Net method, we conduct extensive experiments on two different datasets acquired by UAV-mounted laser scanners, and demonstrate the superiority of our proposed method in individual power line extraction.

The remainder of the whole paper is organized as follows. Section 2 introduces the related research on routine power line inspection based on remote sensing data. Section 3 expounds the procedure of our proposed automated individual power line extraction method. Section 4 demonstrates the effectiveness of our proposed method through the extensive experiments on the point clouds collected by different UAV laser scanners. The paper is concluded in Section 5.

2. Related Work

To reduce the costs and labor involved in power line inspection and achieve intelligent power line inspection, numerous researchers have focused on developing various technologies. In this section, we introduce the related works on power line inspection, specifically focusing on two categories: image-based power line inspection and point-cloud-based power line inspection.

2.1. Image-Based Power Line Inspection

Image-based methods still play a key role in the area of power line inspection. In collaboration with machine vision, Chen et al. [18] explored the Radon transform for automatically achieving the power line extraction in high-resolution remote sensing imagery. To recognize power lines in aerial images, Yetgin and Gerek [19] introduced a new strategy to obtain discrete feature extraction by applying the cosine transform. Building upon the local-to-global concept, Song and Li [20] presented a sequential power line extraction method in two criteria, i.e., in the local criterion, power lines were segmented through morphological filtering and edge maps by calculating the matched filters and the first-order Gaussians derivatives, respectively; in the global criterion, the entire and compact power lines are formed and refined by designing a graph cut-based model. Based on the probabilistic graph model, Zhao et al. [21] proposed a power line extraction method for aerial images in three steps. Firstly, a line detector was proposed to extract line segments, which were treated as basic units to construct a graph model. Then, based on the constructed graph model, a Markov random field [22] was introduced to refine the extracted power line segments. Finally, the whole power line was obtained by fitting an envelope line. To achieve automatic power line inspection, Chang et al. [23] proposed a Convolutional Generative Adversarial Network (cGAN) model to integrate a deep-learning-based semantic segmentation network with a lightweight Generative Adversarial Network [24] for power line extraction. In the proposed cGAN model, the generator was responsible for encoding the area images by generating the synthetic data, while the discriminator distinguished whether the data was from real area images. Based on the adversarial learning between the generator and discriminator, the generator could extract a discriminative feature for power line inspection. Due to the reliability and all-weather operational capability of

millimeter-wave radar systems, Sarabandi et al. [25] proposed a statistical polarimetric detection algorithm that utilized coherence between polarized components, demonstrating improved power line mapping in SAR images with low-grazing incidence. To prevent power-line-strike accidents for low-flying aircrafts, Ma et al. [26] designed a set of features to describe the Bragg pattern for the reliable recognition of power lines in SAR videos.

2.2. Point-Cloud-Based Power Line Inspection

The existing related studies on power line inspection mainly focus on the manually designed descriptors [15,27]. These methods obtained the segmentation results of power lines and power towers by extracting the local geometric features of the targets through manually designed operators. Jung et al. [27] computed the geometric features of each voxel and extracted power lines from point cloud data using a voxel-based hierarchical approach. Shen et al. [15] partitioned the original space into multiple subspaces and segmented power lines and towers using multiple height thresholds. To achieve the power line extraction from point cloud data, Xu et al. [28] proposed a three-step method by exploiting maximum a posteriori probability and linear structural information. Guo et al. [29] jointly leveraged geometric characteristics and echo information of the laser scanning point cloud to obtain a fused feature, and achieved the classification for power line extraction through the JointBoost classifier. In order to improve the robustness of the power line segmentation, Wang et al. [30] designed a multi-scale cylinder neighborhood to capture a compact spatial structure feature. Some methods transformed the unordered point cloud into regular geometric data structures, such as three-dimensional voxels and two-dimensional images, and introduced the methods of image processing to perform power line extraction tasks. Guo et al. [29] combined similarity detection and random sample consensus to detect data distribution characteristics and estimate power line models. Yang et al. [31] first transformed point clouds into 3D voxels as operating units, and then integrated Laplacian smoothing [32] with Markov random fields to obtain a locally continuous and globally optimal result for power line extraction.

On one hand, although image-based studies have shown their promising performance in certain scenarios, their performances are easily influenced by the intrinsic deficiency brought optical imaging systems such as occlusion, lighting variations, lack of geometric information, etc. On the other hand, although traditional point-cloud-based methods have developed various manually designed descriptors, the latent patterns implied in the point clouds still cannot be accurately captured. Moreover, traditional point-cloud-based methods are heavily influenced by manual setup and threshold settings, which limits their generalizability.

3. Materials and Methods

3.1. An Overview of EM-Net

As shown in Figure 1, the multi-branch network architecture of the proposed EM-Net mainly contains three components: the backbone network, the power line and power tower extraction branch, and the individual power line feature learning branch. The main benefit of designing the proposed EM-Net as a multi-branch network is to reduce the massive requirements of annotated training samples. Specifically, the backbone network is responsible for encoding a convolutional feature for the large-scale point cloud scenes. The backbone network is shared by the two branches. The power line and power tower extraction branch is responsible for classifying the points into three categories, i.e., power line, power tower, and others. The individual power line feature learning branch is responsible for generating the discriminative embeddings to guarantee the separation of individual power lines.

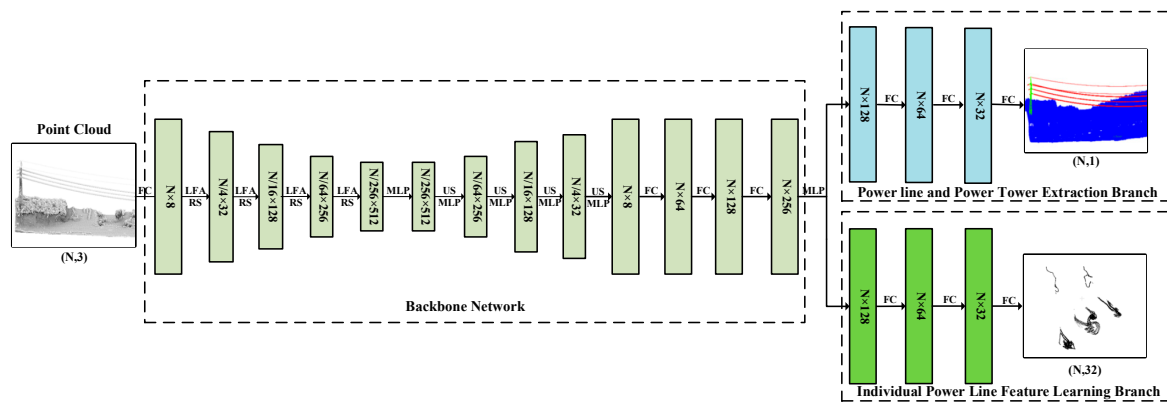


Figure 1. Illustration of the network architecture of the proposed EM-Net. Here, N represents the number of points in the input point cloud. FC, LFA, RS, US, and MLP, represent Fully Convolution, Local Feature Aggregation, Random Sampling, Up Sampling, and Multilayer Perceptron, respectively.

During the training phase of the network, the single power line extraction branch ignores points that do not belong to the power line category when calculating the loss. In the inference phase of the network, the single power line extraction branch computes point embeddings for all points, while the power line segmentation branch assigns a categorical label to each point. Finally, only the point embeddings classified as belonging to the power line category in the segmentation branch are retained.

3.2. The Backbone Network

To extract power lines and power towers in large-scale point clouds, it is extremely important to design a proper backbone network for efficiently capturing the local and global contexts. Here, to consider massive 3D points in the collected outdoor 3D point cloud data, we leverage RandLA-Net [17] as the backbone network. The RandLA-NET can achieve efficient and rapid feature extraction for large-scale point clouds. Specially, RandLA-Net uses random sampling to reduce the number of points in each layer, thereby reducing computational costs and speeding up the feature extraction procedure. Moreover, as shown in Figure 1, the RandLA-Net network mainly consists of Encoder layers and four Decoder layers. In the Encoder layers, point cloud features are successively down-sampled from the original $(N, 8)$ through the Local Feature Aggregation (LFA) module and Random Sample (RS) to $(N/4, 32)$, $(N/16, 128)$, $(N/64, 256)$, and $(N/256, 512)$, where N represents the number of points. Here, the LFA module is used to aggregate local features and reduce information loss caused by random sampling. The LFA module is a residual structure composed of Local Spatial Encoding (LocSE) and Attentive Pooling (AP). In the LocSE module, the center point, k nearest neighbor points, and distance vectors between the center point and neighbor points are concatenated. The new abstracted feature is obtained through a layer of MLP convolution. The AP modules introduce an attention mechanism to calculate the feature contribution weights of each neighboring point, and ultimately aggregate the feature of the center point. In the decoder stages, features are up-sampled to $(N/64, 256)$, $(N/16, 128)$, $(N/4, 32)$, and $(N, 8)$ by using MLP. To facilitate better feature input into the dual branches, we utilize three fully connected layers to output features as $(N, 256)$.

3.3. The Power Line and Power Tower Extraction Branch

The task of the power line and power tower extraction branch is to classify the points into three categories such as power line, power tower, and others. In this branch, we design three fully connected layers whose neurons are 128, 64, and 32, respectively. In fact, there is a severe category imbalance problem in the collected point cloud scenes. Specifically, the number of three-dimensional points for power lines and power towers in the scene is much smaller than other categories. This imbalance can lead to a bias in

deep-learning networks during training, causing the network to classify power lines and power towers as other categories. Therefore, we introduce a weighted cross entropy loss L_{WCE} into backpropagation to update the training network and effectively train the deep network model in the presence of data imbalance. The Weighted Cross Entropy (WCE) loss is an extension of the traditional cross entropy, where a weight coefficient is added to account for the contribution of classes with smaller proportions in the dataset. We calculate the weighted cross entropy loss L_{WCE} as follows:

$$L_{WCE} = - \sum_{m=1}^M w_m y_m \log(p_m) \quad (1)$$

$$w_m = \frac{1}{\frac{N_m}{N} + \rho} \quad (2)$$

where w_m denotes the calculated weight for category m . N and M represent the number of points and categories in point clouds, respectively. N_m represents the number of points in the predicted category m . y_m represents the one-hot vector for the predicted category m . p_m is the predicted probability of category m . Integrating the WCE loss into the EM-Net allows us to address data imbalances and achieve effective training, even in scenarios where certain classes have significantly fewer instances compared to others. To address scenarios where power lines or power towers are absent, we set ρ to 0.02, thereby preventing the denominator of the weight w_m from reaching zero.

3.4. The Individual Power Line Feature Learning Branch

Addressing the diverse spatial distances between different power lines and the interruptions caused by occlusions is challenging when relying on the original XYZ coordinates or manually crafted feature descriptors. Therefore, in the proposed EM-Net, the individual power line feature learning branch aims to generate a distinctive embedding feature for distinguishing 3D points belonging to the different power lines. We prefer that in the learned embedding feature space, the embeddings of points belonging to the same power line should be located as close as possible, while the embeddings of points from different power lines should be located as far as possible. Moreover, because the number of power lines is often unknown, the designed branch must be suitable for an arbitrary number of power lines. Therefore, inspired by the image-based instance segmentation [33], we propose to design a Discriminative Loss L_{Disc} to train the individual power line feature learning branch as follows:

$$L_{var} = \frac{1}{|C|} \sum_c \frac{1}{N_c} \sum_{i=1}^{N_c} [\|\mu_c - x_i\| - \delta_v]_+^2 \quad (3)$$

$$L_{dist} = \frac{1}{|C|(|C|-1)} \sum_{c_A} \sum_{c_B} [\delta_d - \|\mu_{c_A} - \mu_{c_B}\|]_+^2 \quad (4)$$

$$L_{reg} = \frac{1}{|C|} \sum_c \|\mu_c\| \quad (5)$$

$$L_{Disc} = \alpha \cdot L_{var} + \beta \cdot L_{dist} + \gamma \cdot L_{reg} \quad (6)$$

where C represents the set of power lines in the point cloud scene. $|C|$ gives the number of power lines in C . N_c denotes the number of points belonging to power line c . In practice, C and N_c are only required during the training procedure to learn the discriminative feature descriptions for 3D points belonging to different power lines. x_i and μ_c represent the embedding of 3D point i and the point center of power line c , respectively. $\|\cdot\|$ denotes the L2 distance. $[x]_+^2$ outputs the maximum of the value of x and 0. L_{var} , L_{dist} , and L_{reg} represent the variance term, the distance term, and the regularization term, respectively. Specifically, L_{var} aims to encourage the distance between points belonging to the same power line in the embedding space to not exceed threshold δ_v . L_{dist} encourages the distance

between the embeddings of point centers from different power lines in the feature space to be larger than a predefined margin δ_d . L_{reg} intends to keep all clusters as close as possible to the origin for maintaining the bounded activations. Equation (9) computes the overall loss where α , β , and γ are hyperparameters which give the weight of the variance term, the distance term, and the regularization term, respectively.

3.5. An Arbitrary Number of Individual Power Line Extraction

In Section 3.4, we generate the discriminative embedding of points belonging to the power lines by applying the individual power line feature learning branch. To achieve the unsupervised clustering of an arbitrary number of power lines, we employ the Mean-Shift clustering algorithm [34] to cluster the point embedding and extract the individual power line. Besides the fact that Mean-Shift clustering is an unsupervised clustering method, it does not require the predefinition of the number of clusters. Specifically, the algorithm starts by randomly selecting data points as initial cluster centroids. Then, it iteratively updates these centroids to converge towards the densest regions of the data distribution. The update process is based on the concept of mean-shift, which involves computing the mean of the data points within a certain neighborhood around each centroid. In each iteration, for every data point, a window is defined around the current centroid. The size of the window determines the bandwidth parameter of the algorithm, influencing the extent of the neighborhood considered for each centroid. Because we encourage the EM-Net to distinguish the learned features of different individual power lines according to the value of δ_v at the training stage, we set the value of the bandwidth equal to δ_v in practice. Within this window, the mean-shift vector is calculated by computing the mean of the data points weighted by their similarity to the current centroid. After computing the mean-shift vectors for all data points, the centroids are updated by shifting them towards the directions of the mean-shift vectors. This process is repeated until convergence is reached, typically when the centroids stop moving significantly or a maximum number of iterations is reached.

Once the algorithm converges, each data point is assigned to the nearest centroid, forming clusters based on their proximity. The 3D points clustered within the same cluster are conclusively classified as belonging to an individual power line.

4. Experiments

4.1. The Study Area and Dataset

To demonstrate the effectiveness of the proposed EM-Net on extracting an arbitrary number of individual power lines from point cloud scenes, the qualitative and quantitative evaluations are implemented on two datasets, i.e., Datasets I and II. The point clouds in Datasets I and II are acquired from distinct locations utilizing the HawkScan X3 unmanned aerial vehicle (UAV) manufactured by RIEGL in Horn, Austria. Equipped with a laser scanner boasting an accuracy of 2 cm and a point density of 200 points per square meter, this system ensures precise and dense data collection. The used UAV flew at an altitude of 150 m with a speed of 24 km/h, and it achieved a maximum scanning angle of 70° at a frequency of 700 kHz. The total length of point clouds in Dataset I and II was approximately 13 km and 9 km, respectively. For dataset I, we divided the point clouds into 30 segments, each with a length of 400 m. For dataset II, we similarly divided it into 20 segments, each with a length of 400 m. As shown in Figure 2a,b, to validate the performance on power line and power tower extraction, we manually classified the points into three categories, i.e., power lines, power towers, and others. As shown in Figure 2c,d, to validate the performance on individual power line extraction, we manually assigned different category labels to the points belonging to different powerlines. The number of power lines in Datasets I and II ranged from four to ten. In addition, the discontinuous power lines commonly existed in used Datasets I and II.

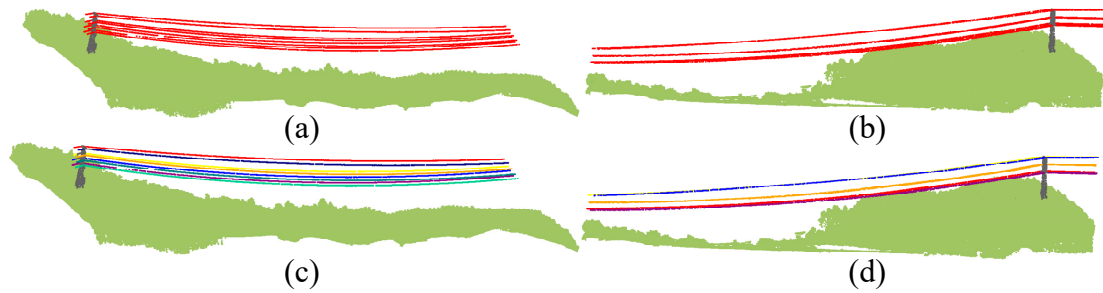


Figure 2. Examples of the point clouds in Dataset I and II. Specifically, (a,b) illustrates the annotations of power lines, power towers, and others in Dataset I and II, respectively. (c,d) illustrates the annotations of different individual powerlines in Dataset I and II, respectively. Here, different color represents different categories.

4.2. Implementation Details

In the proposed EM-Net, the designed two branches are alternatively optimized. Specifically, at each iteration, we first train the power line and power tower extraction branch to minimize the weighted cross entropy loss. Then, we train the individual power line feature learning branch to minimize the discriminative loss. Here, the distance thresholds δ_v and δ_d used in Equations (3) and (4) are empirically set to 1.0 and 0.5, respectively. The hyperparameters α , β , and γ are set to 1.0, 1.0, and 0.001, respectively. Once the training procedure converges, we can obtain the trained EM-Net to implement power line and power tower extraction and accomplish the individual power line extraction.

For training the EM-Net, the initial learning rate of the network is set to 0.01 with a decay rate of 0.95. The batch size and the training epochs are set to 4 and 100, respectively. The EM-Net is coded with Python 3.6 and TensorFlow 2.6.1. All experiments are executed on a workstation whose GPU, CPU, and operating system are 3090ti, Intel i9-12900K, and Ubuntu 18.04, respectively.

4.3. Experiments and Discussion

4.3.1. Evaluation Metrics

To assess the performance of extracting the individual power lines, we used three evaluation metrics including precision, recall, and F1-score. Specifically, the used evaluation metrics are calculated as follows:

$$\text{precision} = \frac{\text{TP}}{\text{TP} + \text{FP}} \quad (7)$$

$$\text{recall} = \frac{\text{TP}}{\text{TP} + \text{FN}} \quad (8)$$

$$\text{F1 - score} = \frac{2 * \text{precision} * \text{recall}}{\text{precision} + \text{recall}} \quad (9)$$

where TP represents the point correctly identified as individual powerline in ground truth. FN and FP represent the point incorrectly identified as negative samples and positive samples, respectively. The precision value indicates correctly recognized individual power lines. A higher recall value indicated a higher ability to find all the points belonging to individual power lines. The F1-score provided a comprehensive consideration of precision and recall.

4.3.2. Individual Powerline Extraction

We conducted extensive experiments to evaluate the performance of the proposed EM-Net on extracting individual powerlines in point clouds. Table 1 records the experimental results of the proposed EM-Net on extracting individual powerlines by using five-fold cross-validation. To implement the five-fold cross-validation, we divided Dataset I and II into five

equal parts on average. As recorded in Table 1, the proposed EM-Net obtained a satisfactory performance on all three measurements for each split. Moreover, the proposed EM-Net achieved average precision, recall, and F1-score at 0.986, 0.975, and 0.981, respectively. This exhibits how the proposed method has a promising performance on extracting individual power lines in point clouds. Furthermore, Figure 3 presents the visualization of the extraction results obtained by applying our proposed EM-Net. As shown in Figure 3, although the number of power lines varied, the proposed EM-Net could not only accurately extract power lines and power towers, but could also distinguish 3D points belonging to different power lines. This further exhibits the excellent performance of the proposed EM-Net on extracting an arbitrary number of individual power lines in point clouds.

Table 1. The experimental results of five-fold cross validation of the proposed EM-Net on individual power line extraction.

Datasets	Precision	Recall	F1-Score
Split I	0.992	0.979	0.985
Split II	0.990	0.984	0.987
Split III	0.985	0.970	0.978
Split IV	0.981	0.965	0.973
Split V	0.984	0.977	0.981
Avg	0.986	0.975	0.981

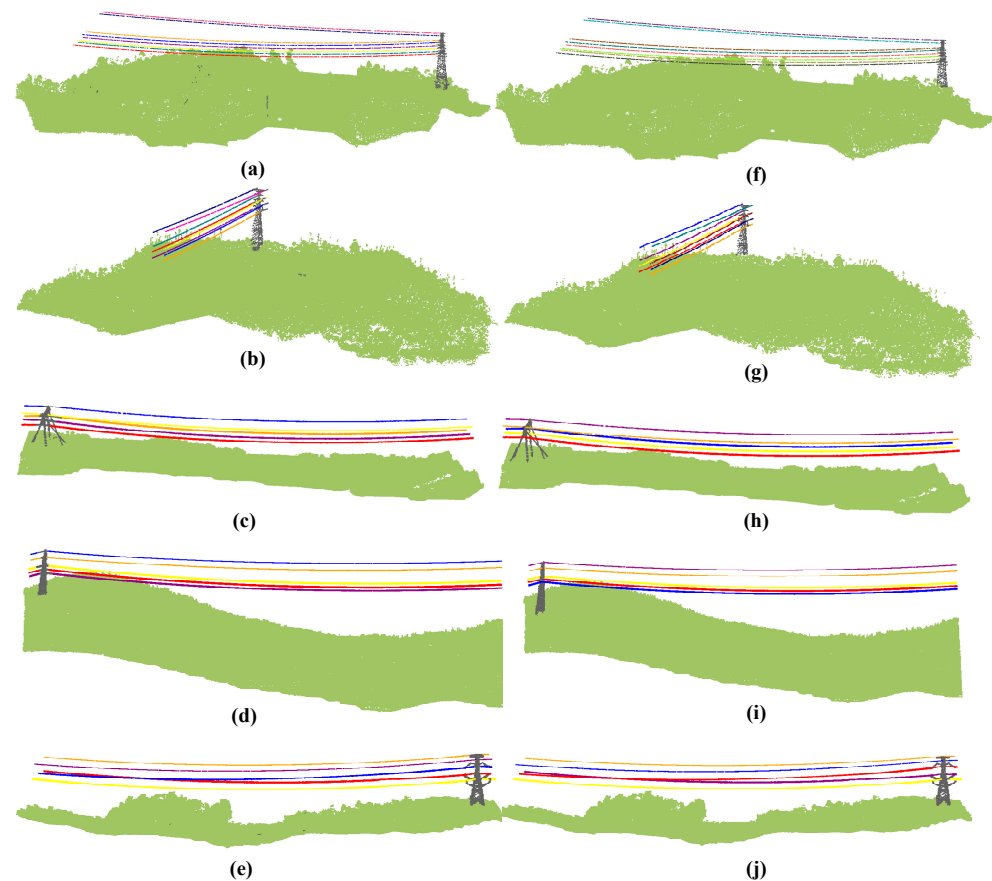


Figure 3. The visualization of the results of the proposed EM-Net on extracting individual power lines from point clouds. Specifically, (a–e) and (f–j) represent the extraction results obtained by the proposed EM-Net and the ground truth, respectively. Here, different colors indicate different individual power lines.

4.3.3. A Comparative Experiment

To demonstrate the superior performance, we also compared the proposed EM-Net with different methods including DBSCAN [35], RANSAC [16], and RECONSTRUCT [27]. Specifically, the DBSCAN method first exploits RandLA-Net to extract power line points, then leverages the DBSCAN algorithm to spatially cluster the extracted power line points, and finally treats each cluster as a single power line. The RANSAC method mainly leverages the most widely used robust RANSAC estimator [36] to estimate the power line for distinguishing points belonging to different individual power lines. The RECONSTRUCT method extracts the powerline points by (1) removing the points belonging to the ground and unwanted objects and (2) refining the powerline points by denoising, clustering, and reconstructing.

Table 2 records the comparative results of the EM-Net against other methods. As shown in Table 2, the EM-Net achieved the highest score for precision, recall, and F1-score. Moreover, we provide the visualization of results obtained by different methods in Figure 4. As shown in Figures 4 and 5, the DBSCAN, RANSAC, and RECONSTRUCT methods all had varying degrees of misclassification, thus our proposed EM-Net obtained the accurate classification, which demonstrates the superior performance of EM-Net on extracting individual power lines from point clouds collected by UAV-mounted laser scanners. Specifically, as region 1# shows in Figure 4, when the power line was interrupted due to occlusion, the DBSCAN and RECONSTRUCT methods often incorrectly classified one line as two lines. Moreover, as region 2# shows in Figure 5, when the power line crossed the power tower, the DBSCAN and RECONSTRUCT methods often failed to recognize the points belonging to a single power line. However, in both region 1# and 2#, our proposed EM-Net accurately identified individual power lines. This is because, compared to the other methods which adopt the handcrafted feature descriptors, our proposed EM-Net designed a discriminative loss to automatically learn about effective feature descriptions, which is beneficial for the individual power line extraction.

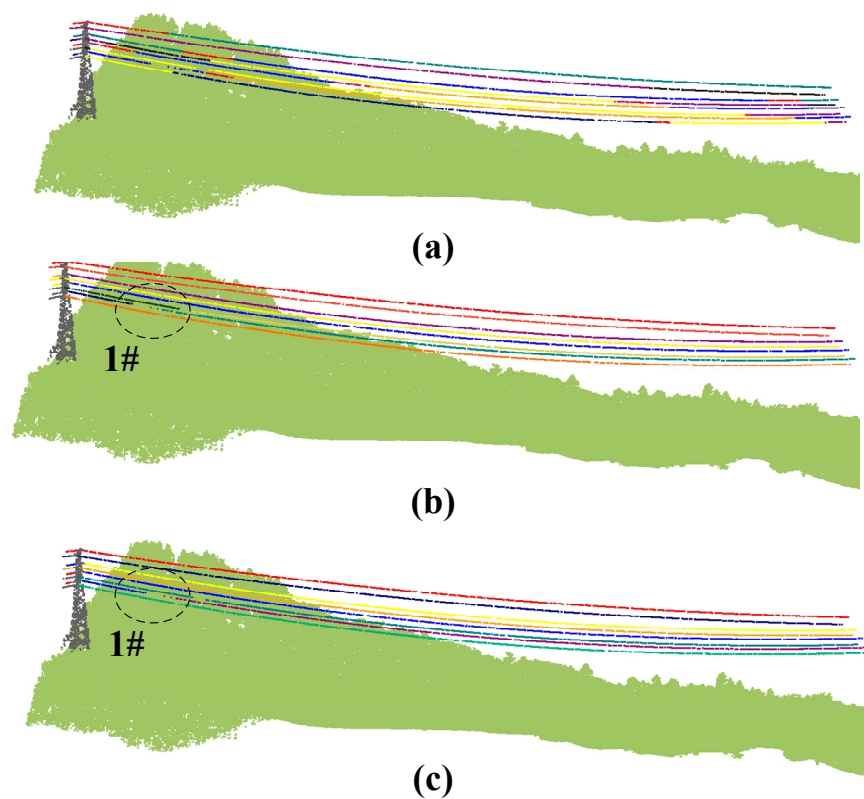


Figure 4. Cont.

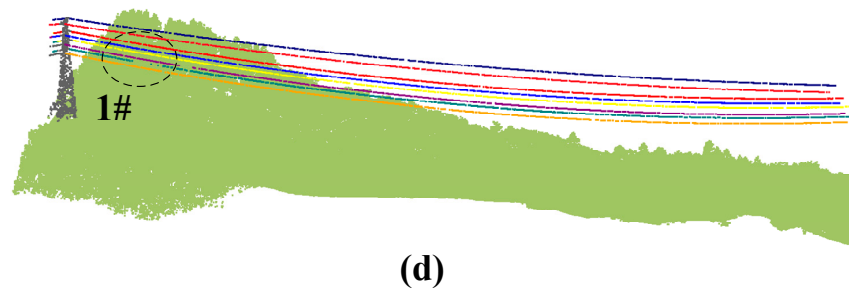


Figure 4. The visualization of the results obtained by the different methods on extracting individual power lines on scene I. Specifically, (a–d) are results obtained by the RANSAC, DBSCAN, RECONSTRUCT and EM-Net (ours), respectively.

Table 2. The comparative results of the EM-Net against other methods.

Methods	Precision	Recall	F1-Score
RANSAC	0.986	0.581	0.731
DBSCAN	0.868	0.657	0.748
RECONSTRUCT	0.986	0.941	0.963
EM-Net	0.987	0.975	0.981

4.4. Discussion

To evaluate the significance of the weighted cross-entropy loss function, we conducted a comparative analysis with the conventional Cross-Entropy (CE) loss. According to [37], we used precision, recall, and F1 scores as metrics. Considering the application of our Weighted Cross-Entropy (WCE) in the branch dedicated to extracting power lines and towers, we investigated its influence on the extraction process. As presented in Tables 3 and 4, the weighted cross-entropy exhibits a conspicuous enhancement in the extraction performance on extracting power lines and power towers. Notably, a remarkable nearly 7% and 1% boost in recall was observed for the power towers and power lines, respectively. When utilizing the weighted cross-entropy, we observed precision, recall, and F1 scores of 95.11%, 96.86%, and 95.97%, respectively for the power tower. Remarkably, for the power line category, all metrics exceeded 99%.

Table 3. The experimental results of power tower extraction of the proposed EM-Net with WEC loss and EC loss.

Loss	Precision	Recall	F1-Score
CE loss	95.44	89.97	92.63
WCE loss	95.11	96.86	95.97

Table 4. The experimental results of power line extraction of the proposed EM-Net with WEC loss and EC loss.

Loss	Precision	Recall	F1-Score
EC loss	99.52	98.83	99.17
WEC loss	99.31	99.51	99.41

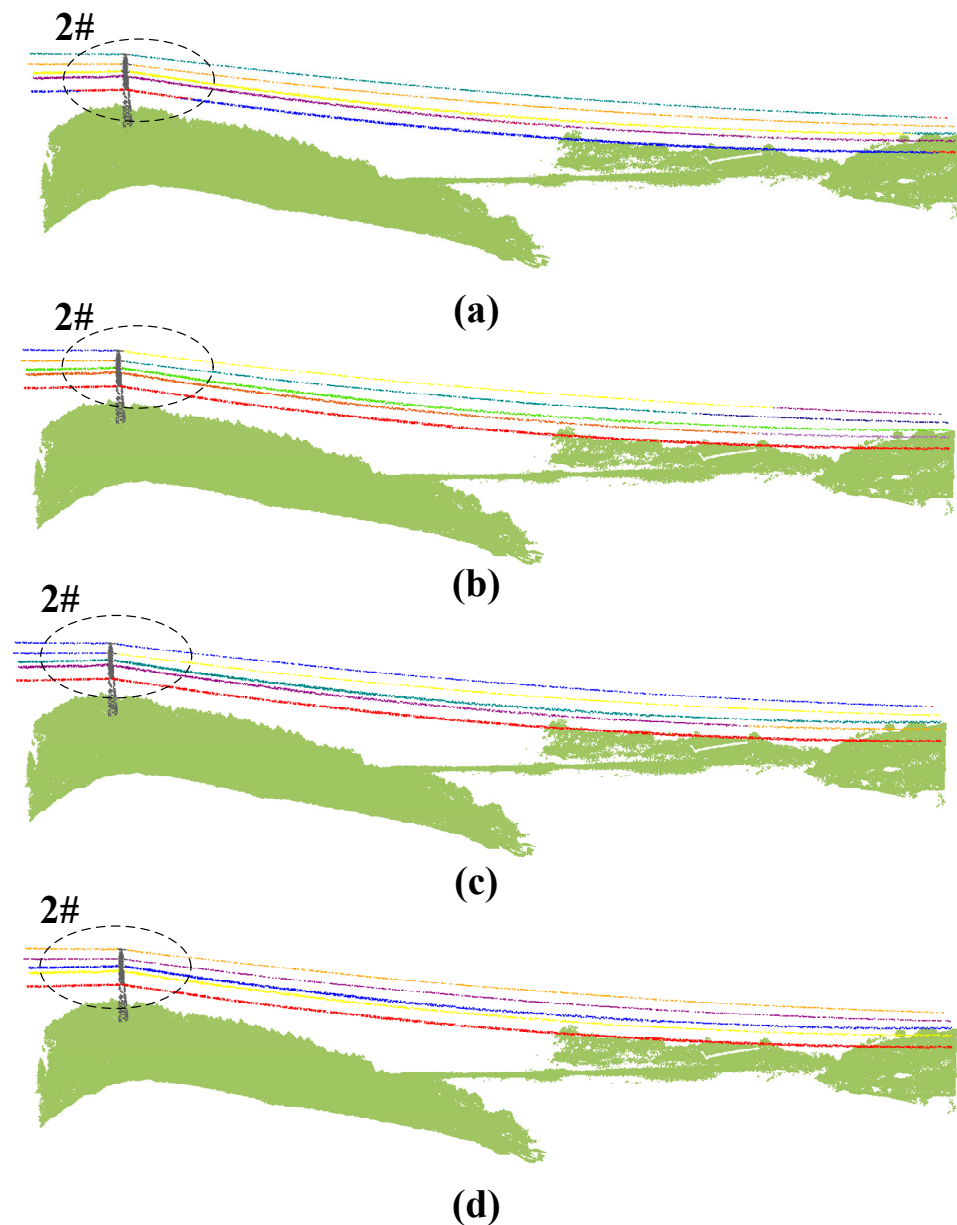


Figure 5. A visualization of the results obtained by the different methods of extracting individual power lines on scene II. Specifically, (a–d) show results obtained by RANSAC, DBSCAN, RECONSTRUCT and EM-Net (ours), respectively.

To analyze the importance of the bandwidth value on the individual power line extraction, we implement the proposed EM-Net under different bandwidth values. Table 4 records the results of the proposed EM-Net of different bandwidth values at 0.5, 0.8, 1.0, 1.2, and 1.5. As recorded in Table 5, when the bandwidth value ranged from 0.5 to 1.0, the scores of all the measurements slightly increased. When the bandwidth value ranged from 1.0 to 1.5, the value of precision, recall, and F1-scores slightly decreased. When the bandwidth value was set at 1.0, the value of F1-scores reached the highest value at 0.965. This reflects that the proposed EM-Net can obtain the superior performance when we only set the bandwidth value equal to δ_v , which was set at 1.0. This is because the EM-Net learns that the feature distance between 3D points belonging to the same power line in the embedding space should not exceed the threshold δ_v .

Table 5. The experimental results of the proposed EM-Net under different bandwidth values.

Bandwidth	Precision	Recall	F1-Score
0.5	0.983	0.916	0.949
0.8	0.995	0.809	0.893
1.0	0.967	0.964	0.965
1.2	0.973	0.942	0.957
1.5	0.974	0.858	0.912

5. Conclusions

To effectively extract power lines and differentiate points from different power lines in point clouds obtained from UAV-mounted laser scanners, this paper presents a novel multi-branch neural network called EM-Net. The multi-branch architecture of EM-Net allows for the effective learning of latent feature embeddings in unorganized 3D points. Furthermore, a discriminative loss function is designed to explicitly guide the feature-learning process in distinguishing points belonging to different power lines. To address imbalanced point clouds' data for training EM-Net, a weighted cross entropy loss is introduced to enhance the ability of EM-Net to classify the minority category. The proposed method has been evaluated on two datasets acquired from UAV-mounted laser scanners at different locations. The qualitative results have demonstrated that our EM-Net achieves the highest scores on individual power line extraction for metrics such as precision, recall, and F1-score at 0.986, 0.975, and 0.981, respectively. These scores surpass those obtained by the DBSCAN, RANSAC, and RECONSTRUCT methods. These results highlight the superior performance of our proposed method in extracting an arbitrary number of individual power lines.

Author Contributions: S.Z.: Methodology, Writing—original draft, Funding acquisition, Conceptualization. Q.L.: Methodology, Writing—review and editing. J.Z.: Conceptualization, Funding acquisition, Writing—original draft. L.L.: Writing—review and editing. C.Z.: Conceptualization, Writing—original draft, Writing—review and editing. G.Z.: Resources, Supervision, Validation. Z.C.: Methodology, Writing—original draft, Writing—review and editing. Y.C.: Funding acquisition, Supervision, Resources, Conceptualization. All authors have read and agreed to the published version of the manuscript.

Funding: This study is funded by the investment oriented technology project “Key Technology Research on Tower and Power Line Extraction Based on 3D LiDAR Point Cloud” of State Grid Siji Location Service Co., Ltd. in Beijing, China (Project No. 546821220006).

Data Availability Statement: The data presented in this study are available on request from the corresponding author. The data are not publicly available due to privacy.

Conflicts of Interest: The Authors Sha Zhu, Chunguang Zhang, Guang Zhao, Lu Li, and Jianwei Zhao were employed by the State Grid Siji Location Based Service Co., Ltd., Beijing, China. Qiang Li was employed by the State Grid Information & Telecommunication Group Co., Ltd., Beijing, China. The remaining authors declare that the research was conducted in the absence of any commercial or financial relationships that could be construed as a potential conflict of interest. The funders had no role in the design of the study; in the collection, analyses, or interpretation of data; in the writing of the manuscript; or in the decision to publish the results.

References

- Matikainen, L.; Lehtomäki, M.; Ahokas, E.; Hyypä, J.; Karjalainen, M.; Jaakkola, A.; Kukko, A.; Heinonen, T. Remote sensing methods for power line corridor surveys. *ISPRS J. Photogramm. Remote Sens.* **2016**, *119*, 10–31. [\[CrossRef\]](#)
- Li, X.; Guo, Y. Application of LiDAR technology in power line inspection. *IOP Conf. Ser. Mater. Sci. Eng.* **2018**, *382*, 052025. [\[CrossRef\]](#)
- Wang, Z.; Gao, Q.; Xu, J.; Li, D. A review of UAV power line inspection. In *Advances in Guidance, Navigation and Control; Lecture Notes in Electrical Engineering*; Springer: Singapore, 2022; pp. 3147–3159.
- Guan, H.; Li, J.; Zhou, Y.; Yu, Y.; Wang, C.; Wen, C. Automatic extraction of power lines from mobile laser scanning data. In *Proceedings of the 2014 IEEE Geoscience and Remote Sensing Symposium, Quebec City, QC, Canada, 13–18 July 2014*.

5. Mills, S.J.; Castro, M.P.G.; Li, Z.; Cai, J.; Hayward, R.; Mejias, L.; Walker, R.A. Evaluation of aerial remote sensing techniques for vegetation management in power-line corridors. *IEEE Trans. Geosci. Remote Sens.* **2010**, *48*, 3379–3390. [[CrossRef](#)]
6. Mclaughlin, R. Extracting transmission lines from airborne LIDAR data. *IEEE Geosci. Remote Sens. Lett.* **2006**, *3*, 222–226. [[CrossRef](#)]
7. Li, Z.; Walker, R.; Hayward, R.; Mejias, L. Advances in vegetation management for power line corridor monitoring using aerial remote sensing techniques. In Proceedings of the 2010 1st International Conference on Applied Robotics for the Power Industry, Montreal, QC, Canada, 5–7 October 2010; pp. 1–6.
8. Luo, Y.; Yu, X.; Yang, D.; Zhou, B. A survey of intelligent transmission line inspection based on unmanned aerial vehicle. *Artif. Intell. Rev.* **2023**, *56*, 173–201. [[CrossRef](#)]
9. Zhang, H.; Wu, L.; Chen, Y.; Chen, R.; Kong, S.; Wang, Y.; Hu, J.; Wub, J. Attention-guided multitask convolutional neural network for power line parts detection. *IEEE Trans. Instrum. Meas.* **2022**, *71*, 1–13. [[CrossRef](#)]
10. Xu, C.; Li, Q.; Zhou, Q.; Zhang, S.; Yu, D.; Ma, Y. Power line-guided automatic electric transmission line inspection system. *IEEE Trans. Instrum. Meas.* **2022**, *71*, 1–18. [[CrossRef](#)]
11. Zhang, H.; Yang, W.; Yu, H.; Zhang, H.; Xia, G.-S. Detecting power lines in UAV images with convolutional features and structured constraints. *Remote Sens.* **2019**, *11*, 1342. [[CrossRef](#)]
12. Li, J.; Yang, B.; Cong, Y.; Cao, L.; Fu, X.; Dong, Z. 3D forest mapping using a low-cost UAV laser scanning system: Investigation and comparison. *Remote Sens.* **2019**, *11*, 717. [[CrossRef](#)]
13. Bi, Z.; Wang, L. Advances in 3D data acquisition and processing for industrial applications. *Robot. Comput.-Integr. Manuf.* **2010**, *26*, 403–413. [[CrossRef](#)]
14. Maiellaro, N.; Zonno, M.; Lavallo, P. Laser scanner and camera-equipped UAV architectural surveys. *Int. Arch. Photogramm. Remote Sens. Spat. Inf. Sci.* **2015**, *40*, 381–386. [[CrossRef](#)]
15. Shen, X.; Qin, C.; Du, Y.; Yu, X.; Zhang, R. An automatic extraction algorithm of high voltage transmission lines from airborne LIDAR point cloud data. *Turk. J. Electr. Eng. Comput. Sci.* **2018**, *26*, 2043–2055. [[CrossRef](#)]
16. Gaha, M.; Jaafar, W.; Fakhfekh, J.; Houle, G.; Abderrazak, J.B.; Bourgeois, M. A new lidar-based approach for poles and distribution lines detection and modelling. *Comput. Sci. Inf. Technol.* **2021**, *11*, 85–97.
17. Hu, Q.; Yang, B.; Xie, L.; Rosa, S.; Guo, Y.; Wang, Z.; Trigoni, N.; Markham, A. Randla-net: Efficient semantic segmentation of large-scale point clouds. In Proceedings of the IEEE/CVF Conference on Computer Vision and Pattern Recognition (CVPR), Seattle, WA, USA, 13–19 June 2020; pp. 11108–11117.
18. Chen, Y.; Li, Y.; Zhang, H.; Tong, L.; Cao, Y.; Xue, Z. Automatic power line extraction from high resolution remote sensing imagery based on an improved Radon transform. *Pattern Recognit.* **2016**, *49*, 174–186. [[CrossRef](#)]
19. Yetgin, Ö.E.; Gerek, Ö.N. Automatic recognition of scenes with power line wires in real life aerial images using DCT-based features. *Digit. Signal Prog.* **2018**, *77*, 102–119. [[CrossRef](#)]
20. Song, B.; Li, X. Power line detection from optical images. *Neurocomputing* **2014**, *129*, 350–361. [[CrossRef](#)]
21. Zhao, L.; Wang, X.; Yao, H.; Tian, M.; Jian, Z. Power line extraction from aerial images using object-based markov random field with anisotropic weighted penalty. *IEEE Access* **2019**, *7*, 125333–125356. [[CrossRef](#)]
22. Boykov, Y.; Veksler, O.; Zabih, R. Markov random fields with efficient approximations. In Proceedings of the 1998 IEEE Computer Society Conference on Computer Vision and Pattern Recognition, Santa Barbara, CA, USA, 23–25 June 1998; pp. 648–655.
23. Chang, W.; Yang, G.; Li, E.; Liang, Z. Toward a cluttered environment for learning-based multi-scale overhead ground wire recognition. *Neural Process. Lett.* **2018**, *48*, 1789–1800. [[CrossRef](#)]
24. Goodfellow, I.; Pouget-Abadie, J.; Mirza, M.; Xu, B.; Warde-Farley, D.; Ozair, S.; Courville, A.; Bengio, Y. Generative adversarial networks. *Commun. ACM* **2020**, *63*, 139–144. [[CrossRef](#)]
25. Sarabandi, K.; Park, M. Extraction of power line maps from millimeter-wave polarimetric SAR images. *IEEE Trans. Antennas Propag.* **2000**, *48*, 1802–1809. [[CrossRef](#)]
26. Ma, Q.; Goshi, D.S.; Shih, Y.-C.; Sun, M.-T. An Algorithm for Power Line Detection and Warning Based on a Millimeter-Wave Radar Video. *IEEE Trans. Image Process.* **2011**, *20*, 3534–3543. [[CrossRef](#)]
27. Jung, J.; Che, E.; Olsen, M.J.; Shafer, K.C. Automated and efficient powerline extraction from laser scanning data using a voxel-based subsampling with hierarchical approach. *ISPRS J. Photogramm. Remote Sens.* **2020**, *163*, 343–361. [[CrossRef](#)]
28. Xu, S.; Wang, R. Power line extraction from mobile LiDAR point clouds. *IEEE J. Sel. Top. Appl. Earth Obs. Remote Sens.* **2019**, *12*, 734–743. [[CrossRef](#)]
29. Guo, B.; Huang, X.; Zhang, F.; Sohn, G. Classification of airborne laser scanning data using JointBoost. *ISPRS J. Photogramm. Remote Sens.* **2015**, *100*, 71–83. [[CrossRef](#)]
30. Wang, Y.; Chen, Q.; Liu, L.; Zheng, D.; Li, C.; Li, K. Supervised classification of power lines from airborne LiDAR data in urban areas. *Remote Sens.* **2017**, *9*, 771. [[CrossRef](#)]
31. Yang, J.; Kang, Z. Voxel-based extraction of transmission lines from airborne LiDAR point cloud data. *IEEE J. Sel. Top. Appl. Earth Obs. Remote Sens.* **2018**, *11*, 3892–3904. [[CrossRef](#)]
32. Hansbo, P. Generalized Laplacian smoothing of unstructured grids. *Commun. Numer. Methods Eng.* **1995**, *11*, 455–464. [[CrossRef](#)]
33. De Brabandere, B.; Neven, D.; Van Gool, L. Semantic instance segmentation with a discriminative loss function. *arXiv* **2017**, arXiv:1708.02551.
34. Wu, K.-L.; Yang, M.-S. Mean shift-based clustering. *Pattern Recognit.* **2007**, *40*, 3035–3052. [[CrossRef](#)]

35. Birant, D.; Kut, A. ST-DBSCAN: An algorithm for clustering spatial–temporal data. *Data Knowl. Eng.* **2007**, *60*, 208–221. [[CrossRef](#)]
36. Fischler, M.A.; Bolles, R.C. Random sample consensus: A paradigm for model fitting with applications to image analysis and automated cartography. *Commun. ACM* **1981**, *24*, 381–395. [[CrossRef](#)]
37. Luo, H.; Wang, C.; Wen, C.; Chen, Z.; Zai, D.; Yu, Y.; Li, J. Semantic labeling of mobile LiDAR point clouds via active learning and higher order MRF. *IEEE Trans. Geosci. Remote Sens.* **2018**, *56*, 3631–3644. [[CrossRef](#)]

Disclaimer/Publisher’s Note: The statements, opinions and data contained in all publications are solely those of the individual author(s) and contributor(s) and not of MDPI and/or the editor(s). MDPI and/or the editor(s) disclaim responsibility for any injury to people or property resulting from any ideas, methods, instructions or products referred to in the content.